Published in final edited form as:
Cell Tissue Res. 2013 December ; 354(3): . doi:10.1007/s00441-013-1710-y.

Arp2/3 complex inhibitors adversely affect actin cytoskeleton remodeling in the cultured murine kidney collecting duct M-1 cells

Daria V. Ilatovskaya[1,2,*], **Vladislav Chubinskiy-Nadezhdin**[1,*], **Tengis S. Pavlov**[2], **Leonid S. Shuyskiy**[1], **Viktor Tomilin**[1], **Oleg Palygin**[2], **Alexander Staruschenko**[2], and **Yuri A. Negulyaev**[1]

[1]Institute of Cytology, Russian Academy of Sciences, St. Petersburg, 194064, Russia

[2]Department of Physiology, Medical College of Wisconsin, Milwaukee, WI 53226, USA

Abstract

Dynamic remodeling of the actin cytoskeleton plays an essential role in cell migration and various signaling processes in the living cells. One of the critical factors that controls the nucleation of new actin filaments in eukaryotic cells is the actin related protein 2/3 (Arp2/3) complex. Recently, two novel classes of small molecules that bind to different sites on the Arp2/3 complex and inhibit its ability to nucleate F-actin have been discovered and described. The current study was aimed at investigating the effects of CK-0944666 (CK-666) and its analogs (CK-869 and inactive CK-689) on the reorganization of the actin microfilaments in the cortical collecting duct cell line, M-1. We have shown that treatment with CK-666 and CK869 results in the reorganization of F-actin and drastically affects cell motility rate. The concentrations of the compounds used in this study (100-200 μM) neither cause loss of cell viability nor influence cell shape or monolayer integrity; hence the effects of described compounds were not due to the structural side effects. Therefore, we conclude here that the Arp2/3 complex plays an important role in cell motility and F-actin reorganization in M-1 cells. Furthermore, CK-666 and its analogs are useful tools for the investigation of the Arp2/3 complex.

Keywords

Arp2/3 complex; actin filaments; CK-0944666; cell motility

Introduction

Actin is the major constituent of the cytoskeleton that participates in various cellular events including motility, endocytosis, cellular shape support, and protein and organelle trafficking (Collins et al. 2011;Saarikangas et al. 2010;Peleg et al. 2011). In recent years, processes and signaling pathways induced by its reorganization have been thoroughly studied and a variety of cytoskeleton-interacting proteins have been revealed.

It was shown that the actin-related protein 2/3 (Arp2/3) complex in combination with other proteins including N-WASP/WAVE family of proteins (Chen et al. 2010;Lebensohn and Kirschner 2009;Sarmiento et al. 2008), cortactin (Weed et al. 2000;Weed and Parsons 2001)

Corresponding author: Daria V. Ilatovskaya, Medical College of Wisconsin, Department of Physiology, 8701 Watertown Plank Rd., Milwaukee, WI 53226. Phone: 414-955-8382, Fax: 414-955-6546, dilatovskaya@mcw.edu.
*equal contribution

and small G-proteins (Watanabe et al. 2010;Sun et al. 2007;Bosse et al. 2007) is involved in regulation of the actin cytoskeleton nucleation and assembly (Firat-Karalar and Welch 2011;Soderling 2009). The Arp2/3 complex is considered to be a key participant in the formation of a stable multimer of actin monomers that helps stabilize the actin-dimer intermediates and promotes branching of the F-actin filaments (Volkmann et al. 2001). The complex consists of two actin-related proteins named Arp2 and Arp3 (encoded by *ARP2* and *ARP3* genes, respectively), that closely resemble the structure of monomeric actin, and five additional subunits *ARPC1-5* (Pollard 2007;Rouiller et al. 2008). This complex is targeted to the sites of new actin polymerization, binds to the side of the existing filaments, and aligns in a similar manner to an actin dimer (Robinson et al. 2001;Volkmann et al. 2001). Therefore, the Arp2/3 complex nucleates the formation of new filaments that extend from the sides of existing filaments at a 70° angle to form a dense network of the Y-branched F-actin (Rouiller et al. 2008).

Since 1994, when the Arp2/3 had been first characterized in *Acanthamoeba* (Machesky et al. 1994), various cellular processes involving this protein complex have been discovered. It has been shown that inhibition of the Arp2/3 complex results in the control of synaptic plasticity (Nakamura et al. 2011), contributes to the formation of the filopodia (Spillane et al. 2011), regulates endosome shape and trafficking (Duleh and Welch 2010), and is engaged in the mechanism of ion channel regulation by cortactin (Ilatovskaya et al. 2011). The Arp2/3 complex is essential for mesenchymal invasion and formation of invadopodia and lamellipodia (Yamaguchi et al. 2005;Sarmiento et al. 2008). It was reported that invasive cells collected from mouse primary breast tumors in an *in vivo* invasion assay, show an increased expression of Arp2/3 (Wang et al. 2004). Moreover, Arp 2/3 complex contributes to cancer cell migration and invasion in human cancers, including head and neck squamous cell (Kinoshita et al. 2012).

Although there have been considerable amounts of data accumulated on the role of the Arp2/3 complex in cytoskeleton dynamics, its participation in cell motility and formation of actin-based protrusions has been underwhelming. Studies have revealed that disrupting the Arp2/3 inhibited lamellipodia formation (Machesky and Insall 1998;Steffen et al. 2006), however other studies have also shown that 90% knock down of the Arp2/3 complex subunits in mouse fibroblasts had no effect of the lamellipodia formation (di Nardo et al. 2005). In 2012 there were two papers that were published on this subject that provided insights into the Arp2/3 complex's critical role in lamellipodia extension and directional migration. Suraneni et al. showed that ARPC/- fibroblasts were unable to extend lamellipodia and exhibited a strong defect in persistent directional migration (Suraneni et al. 2012). Similarly, stable fibroblastsderived cell lines depleted of Arp2/3 complex lacked lamellipodia and showed defective random cell motility that relied on a filopodia-based protrusion system (Wu et al. 2012). It is clear from these studies that depletion of Arp2/3 affects lamellipodia formation. The current study provides support to the fact that the Arp2/3 complex is involved in cell motility and lamellipodia formation.

The exact mechanism by which the Arp2/3 complex affects the cell has yet to be determined. Various attempts to chemically activate or inhibit the Arp2/3 complex remain of particular interest. Nolen and colleagues have identified and characterized novel small molecule inhibitors of the Arp2/3 complex. The authors studied different modifications of potential Arp2/3 inhibitors that were initially discovered by screening a library of over 400,000 possible molecules (Nolen et al. 2009). CK-0944636 (abbreviated CK-636) binds to different sites on the Arp2/3 complex and inhibits its ability to nucleate actin microfilaments. A compound CK-0944666 (abbreviated CK-666) has a fluorobenzene rather than the thiophen ring of CK-636 and was described to be a better inhibitor of actin polymerization that binds more tightly than the originally identified CK-636. Recently, the

crystal structure of CK-666 bound to Arp2/3 complex has been reported, which revealed that CK-666 binds between the Arp2 and Arp3 subunits to stabilize the inactive conformation of the complex (Baggett et al. 2012;Nolen et al. 2009).

CK-666 was recently used to study the contribution of the Arp2/3 complex and actin filaments to mouse oocyte division and cytokinesis (Sun et al. 2011). Disruption of the Arp2/3 complex by CK-666 caused failure of the oocyte to asymmetrically divide, failure of the spindle to migrate, and failure of the oocyte to form properly and undergo cytokinesis. In our recent project, we have also utilized CK-666 in studies of ion channels in the epithelial cells. This inhibitor allowed us to identify the Arp2/3 complex's involvement in the regulation of the epithelial Na^+ channel (ENaC) by cortactin. Importantly, cortactin mutants used in our study, including the mutant W22A which is unable to bind Arp2/3 complex, confirmed the findings obtained with this pharmacological agent (CK-666) (Ilatovskaya et al. 2011). Recently there has been published a paper by Hetrick et al, which has provided new insight into determine the mechanism of CK-666 and its analog CK-869. Their data indicated that CK-666 can stabilize the inactive state of the Arp2/3 complex, blocking movement of the Arp2 and Arp3 subunits into the activated filament-like conformation, while CK-869 binds to a serendipitous pocket on Arp3 and allosterically destabilizes the short pitch Arp3-Arp2 interface (Hetrick et al. 2013).

The goal of the current study was to characterize the regulation of cell migration and determine the mechanisms that can regulate cell movement through the actin cytoskeleton remodeling in the kidney cortical collecting duct principal cells. Particularly, we set out to investigate the role of Arp2/3-mediated changes in the actin cytoskeleton. Additionally, we investigated potential side-effects of CK-666 and its active and inactive analogues, which were recently discovered and not intensively characterized. As seen in our studies, 1) inhibition of the Arp2/3 complex with CK-666 rearranged the actin filaments and decreases cell motility rate, and 2) we have shown that this compound represents a useful tool for the investigation of the Arp2/3 complex.

MATERIALS AND METHODS

Cell culture and chemicals

The M-1 mouse kidney principal cell line (Naray-Fejes-Toth et al. 2004) was obtained from the American Type Culture Collection (ATCC, Manassas, VA, USA) and maintained with standard culture conditions (DMEM, 5% FBS, 1x penicillin-streptomycin, 37°C, 5% CO2); cells were reseeded upon confluence every two or three days. All reagents and media were purchased from Fisher Scientific (Waltham, MA, USA) or Biolot (St. Petersburg, Russia), unless noted otherwise. The inhibitor of the Arp2/3 complex CK-0944666 (CK-666) was purchased at Chemdiv (San Diego, CA, USA); CK-689 and CK-896 were purchased from EMD Biosciences (Merck, Whitehouse Station, USA).

Visualization of F-actin with rhodamine-phalloidin staining and image processing

Cells were seeded onto 12-mm round coverslips 24 hours before experiments. Before staining, the cells were washed with PBS and fixed with 3.7% paraformaldehyde. The cells were then treated with 0.1% Triton X-100 for 5 min, washed with PBS, and incubated with 2 μM rhodamine-phalloidin (Sigma-Aldrich, St. Louis, MO, USA) for 15 minutes at 37°C. Stained cells were mounted on glass slides covered with Vectashield mounting medium (Vector Laboratories, Burlingame, CA, USA). After staining, cells were visualized with a Leica TCS SP5 microscope (Leica Microsystems, GmBH, Wetzlar, Germany) using a 100x oil objective. The signal was excited at 543 nm, and the emission was measured at 590 nm. Fluorescent images were processed with the Leica Application Suite (LAS) software (Leica

Microsystems, GmBH, Wetzlar, Germany) and open-source software ImageJ (National Institutes of Health, USA, http://imagej.nih.gov/ij/) as described previously (Karpushev et al. 2010).

Immunocytochemistry

Immunocytochemistry was performed on M-1 cell monolayers. M-1 cells were fixed with 4% paraformaldehyde in PBS. Before antibody incubation, fixed cells were permeabilized with 0.1% Triton X-100 in PBS and then blocked with 10% donkey serum (1 h at 24 °C). The cells were then incubated with the primary rabbit antibodies at 4°C overnight (anti-cortactin H-191, 1:100 (Santa Cruz Biotech), anti-β-catenin 1:100 (Abcam, ab2982), then incubated with Alexa 488-labeled secondary donkey anti-rabbit antibodies (1:300, 40 min at 37°C) and finally incubated with DAPI (0.05 μg/ml) to stain the nuclei. Cells were mounted with Vectashield Mounting Medium (Vector Laboratories) and imaged with a confocal microscope (Leica TCS SP5, Leica Microsystems, GmBH, Wetzlar, Germany).

Cytotoxicity assay

For the 3-(4,5-dimethylthiazol-2-yl)-2,5-diphenyltetrazolium bromide (MTT) cytotoxicity assay, M-1 cells were seeded onto 12-well cluster plates and allowed to grow for at least 1 week to form a monolayer. Full conditioned media with FBS and antibiotics were changed to DMEM media without supplements 1 h before the experiment. 100 or 200 μM of CK-666 or vehicle were added to the media and the cells were incubated for another 2 hrs. After treatment, MTT (Sigma-Aldrich, St. Louis, MO, USA) was added to the media (0.5 mg/mL), and cells were incubated for 4 additional hours. The medium was aspirated and replaced with isopropanol to solubilize the formazan products followed by optical density readings at 570 nm. The cell viability as a percentage of viable cells was calculated from the absorbance values as described previously (Karpushev et al. 2011). Eight replicate wells were recorded for each measurement.

Live cell microscopy

For live cell microscopy, M-1 cells were seeded onto 15 mm round glass coverslips 24 hrs before the experiment, respectively. Coverslips with attached cells were washed with extracellular solution for 5 min before being mounted in a chamber (0.4 ml, RC-25F, Warner Inst.). For time-lapse studies, they were placed in a temperature-, humidity- and CO_2-controlled chamber on the heating stage of a Zeiss Axio Observer Z1 with a 63x/1.40 Plan-Apochromat oil-immersion objective (Carl Zeiss MicroImaging GmbH, Jena, Germany). Micrographs were taken every 3 min for an observation period of 4 hrs with an AxiocamMRm monochrome digital camera.

Motility rate measurements

The motility rate of M-1 cells was determined by a change in the position of the cell center. The values of the cell center position were obtained using a “centroid” function from the standard measurements plugin of ImageJ software from time-lapse images acquired every 3 min. The distance of movement of single cells in 3 min intervals were calculated as the length of displacement vector. The motility rate of at least 8-10 cells were continuously determined on defined cells before (control) and after addition of the compounds to the solution.

To obtain the mean motility rate of the cells, the displacement vectors were averaged on 3 intervals of time: before addition of the compound (vehicle, 2 hrs) and after 1 and 2 hrs. The mean motility rates after treatment were normalized to mean values, calculated for control conditions (vehicle) in each experiment. The parameters of cell motility were calculated

from tracks of cell motion for each experiment. The direction of cell motility was assessed from polar plots as described previously (Cantarella et al. 2009) or from D/T ratio that is the ratio of the shortest direct distance from the starting point of each recording to the end point (D), to the total distance traversed by the cell (T) (Gu et al. 1999).

Wound healing assay

For the wound-healing assay, M-1 cells were cultured in the DMEM media with 10% FBS and seeded on 4-well plates 24 hr before the experiment at density of 2.0×10^5 cells/ml and cultured overnight at 37°C with 5% CO_2. The "wound" was created with a sterile 300 μL pipette tip, then cells were rinsed with PBS and cell medium was changed for the fresh one. For time-lapse studies, the plates were placed in a temperature-, humidity- and CO_2-controlled chamber on the heating stage of a Zeiss Axio Observer Z1 with a 10x/1.40 Plan-Apochromat objective (Carl Zeiss MicroImaging GmbH, Jena, Germany). Micrographs were taken every 1 hr for an observation period of up to 24 hrs with an AxiocamMRm monochrome digital camera. Images were processed with ImageJ (National Institutes of Health, USA, http://imagej.nih.gov/ij/), wound size was calculated as a function of time.

Statistics

All data are reported as mean ± SEM. Data were compared using the Student (2-tailed) *t* test; $p < 0.05$ was considered significant.

RESULTS

The effects of CK-0944666 on actin remodeling in M-1 epithelial cells

The Arp2/3 complex and its role in the rearrangements of the actin cytoskeleton is very important in the polarized monolayer-forming cells. Several lines of evidence suggest that cytoskeletal elements control the apico-basal polarity of the proteins in the epithelial cells, which is critical for the physiological function of these types of cells (Bryant and Mostov 2008;Wilson 2011). Thus, our experiments were performed on polarized epithelial monolayers of the M-1 cells. As it was described by Nolen and colleagues, the IC_{50} values for CK-666 were 5 and 17 μM after 60 min treatment as shown for *Schizosaccharomyces pombe* and *Bos Taurus* Arp2/3 complexes, respectively (Nolen et al. 2009). In our experiments on living cells, we initially started with CK-666 concentrations of 10 and 50 μM. However, we did not observe any significant differences in cytoskeleton dynamics when the cells were incubated with the drug for up to 1 hr (data not shown); thus, in our experiments we tested higher concentrations of 100 and 200 μM. The cells were seeded on glass coverslips one day before the experiment, grown up to 80% confluency and then incubated with CK-666 diluted in the DMEM media without serum and antibiotics in concentrations of 100 μM for 1 or 2 hrs and 200 μM for 2 hrs; corresponding control cells were kept in the DMEM media with the vehicle. Actin microfilaments were stained with rhodamine-phalloidin followed by confocal microscopy analysis.

To confirm that the observed rearrangements of the cytoskeleton caused by the treatment with CK-666 did not result from the side effects of the compound structure and are directly related to the Arp2/3 complex-targeted action of the drug, we tested both potent and inactive analogs of the CK-666. CK-869, a cell-permeable thiazolidinone compound was used as a positive control for CK-666. This compound was also shown to inactivate the Arp2/3 complex, but exhibits different modes of binding compared to CK-666 (Nolen et al. 2009). As a negative control reagent we selected CK-689, a cell-permeable indolyl-methoxyacetamide, which has structural similarity with CK-666 but exhibits no Arp2/3 inhibitory activity (Nolen et al. 2009).

Fig. 1, a-k illustrate representative staining of the actin filaments in control M-1 cells (Fig. 1a-b) and cells treated with CK-666 (100 μM and 200 μM for 2 hrs, Figs. 1de and g-h, respectively). Shown are the fluorescent images at 100x (a, d, g, j) and close-up images at 2.5x digital zoom (b, e, h, k). Inactive analogue CK-689 was tested in M-1 cells at concentrations of 100 μM or 200 μM during 2 hrs of treatment. As shown by the rhodamine-phalloidin staining of M-1 cells in Fig. 1j,k, treatment with 200 μM CK-689 for 2 hrs did not affect the cytoskeleton structure (staining similar to control) (Fig. 1a,b). A typical actin distribution pattern was observed that included intensive ruffling (shown by arrows). Cells treated with CK-666 showed highly concentrated and bundled actin stress fibers. This difference is particularly apparent in the line scans shown in the bottom row below the corresponding images (Fig.1c,f,i,l). These line scans show the fluorescence emissions (normalized to peak values at each time point) from the actin filaments in the areas defined by the white lines for the cells in the middle rows.

Inhibition of the Arp2/3 complex results in reduced lamellipodia formation

Treatment of the cells with CK-666 significantly reduced the number of the cells with lamellipodia (Fig. 2A) indicating the major role of Arp2/3 complex in the formation of these protrusions. Lamellipodia formation was up to 90% decreased after exposure to CK-666 compared to the control cells and cells treated with CK689 as shown in Fig. 2a. Representative images of the rhodamine-phalloidin stained M-1 cells which were used for the calculations of the lamellipodia number are shown in Figs. 2b (control) and 2c (after treatment with 200 μM CK-666 for 2 hr, lamellipodia are pointed with white arrowheads). Additionally, the cells were stained for the lamellipodia marker cortactin by using standard immunocytochemistry methods. Figs. 2d,e show M-1 cells incubated with DMSO (d) or CK-666 for 2 hr (e) and then stained for cortactin. As shown in this figure (the images were taken at the same focal plane), CK-666 significantly decreased the number of lamellipodia compared to control.

CK-666 neither affects monolayer integrity nor is it cytotoxic

Figs. 3a-d illustrate an example of the M-1 cells' movement at different time points before and after treatment with 200 μM CK-666. The effects of CK-666 on the integrity of the M-1 cell monolayer were evaluated at these different time points. We found that treatment with CK-666 did not influence the cell-to-cell interactions and the monolayer remained intact for up to 2 hrs of exposure to the drug (Fig. 3e and close up image f). This was confirmed with the immunofluorescence staining with anti-β-catenin antibodies to visualize the cell-to-cell contacts. As shown in Fig. 3g-h, the staining pattern of the M-1 cells treated with 200 μM CK-666 for 2 hr (h) remains similar to the staining of the control cells (g, incubated with corresponding amount of the solvent - DMSO) demonstrating that cell-to-cell contacts are still intact. Control experiments (immunofluorescence staining without primary antibodies) did not reveal any staining (data not shown).

To exclude the possibility that the effects of CK-666 on M-1 cells were mediated by a cytotoxic effect, we analyzed the effects of CK-666 on the morphology and viability of these cells. An MTT cytotoxicity assay was perfomed to assess any potential cytotoxic effect of CK-666. Supplementary Fig. S1 summarizes viability of the M-1 cells treated with CK-666. Cytotoxicity was not detected neither when M-1 cells were treated with 100 or 200 μM of CK-666 for 2 hrs.

Treatment with CK-666 significantly reduces M-1 motility rate

To determine whether CK-666, CK-869, or its inactive analogue CK-689 affected cell motility, M-1 cells were seeded onto glass coverslips and grown to 60% confluence one day before the experiments were to be performed. The cells were first treated with 200 μM of

CK-666 and CK-689 for 2 hrs. For assessment of cell motility, a series of time-lapse images were acquired every 3 min over 4 hrs and subsequently analyzed. Fig. 4 shows cell motility from cells treated with vehicle, CK-666 and CK-689. As demonstrated in the representative images, CK-666 significantly reduced the distance travelled by the cells, whereas vehicle and inactive CK-689 did not affect these parameters.

Fig. 5 shows the changes in cell motility rate after treatment with 200 μM CK-666 and CK-689. Motility rate was significantly reduced after inhibition of the Arp2/3 complex with CK-666 compared to the limited effects of CK-689. Similarly, treatment of M-1 cells with CK-869 (200 μM) over 2 hrs resulted in substantial rearrangements of the actin cytoskeleton structure (supplementary Fig. S2); the F-actin distribution pattern was changed similarly to that of the cells treated with CK-666 (Fig. 1). The Factin organization pattern after treatment produced highly bundled actin stress fibers. Motility rate was also significantly lowered compared to vehicle.

The direction of cell motility was also assessed from D/T ratio. The D/T ratio was calculated in order to assess the parameters of cell motility after treatment with CK666 and CK-689. D is defined as the shortest distance between the starting and ending points of the cell motion track, and T is the sum of all distances travelled by cells during the whole interval of observation. D/T ratios were not changed after treatment with CK666 or the negative control CK689, demonstrating the random nature of cell movement (Fig. S3a). The polar plots supported the observation of random, non-directional cell motion as the graphs are almost round-shaped (Fig. S3b). Thus, the treatment of cells with CK-666 and CK-689 had no effect on the D/T ratio or polar plot distribution indicating that CK and its analogs did not change the motility parameters. Therefore, we can conclude that CK-666 does not affect the directionality of cell movement nor does it affect monolayer integrity.

Wound healing assay was performed in order to assess the motility of the M1 cells in the presence of CK-666 or vehicle (in control). Fig. 6,a-f shows 3 images from different time points of the representative wound-healing assay (first image, then 7 h and 14 h after the beginning of the experiment) of the untreated cell monolayer (a,-c) and after treatment with 200 μM CK-666 (d-f). Averaged wound size (normalized to the starting point) as a function of time is shown on Fig. 6g. As clear from the graph, the wound in control heals significantly more effectively than during the treatment of CK-666. Representative videos corresponding to the images shown in Fig. 6a-f can be found in supplementary material (Video S1A and Video S1B correspond to control and CK-666 treated wounds, respectively).

DISCUSSION

In this research, we tested novel inhibitors of the Arp2/3 complex, CK-666 and its analogues, on cell motility and cytoskeleton organization in the immortalized mouse cortical collecting duct cell line, M-1. As seen from our data and from previously published data (Ilatovskaya et al. 2011), CK-666 caused cytoskeleton rearrangements that were associated with the inhibition of the Arp2/3 complex. Sun and colleagues utilized 0.5 mM CK-666 for up to 12 hrs to study the expression and functions of the Arp2/3 complex during mouse oocyte meiotic maturation. This group reported that this concentration resulted in various effects including failure of the oocyte to asymmetrically divide, failure of the spindle to migrate, and failure of the oocyte to form properly and undergo cytokinesis (Sun et al. 2011). We did not test such high concentrations in our experiments. We propose that the concentrations and the duration of time of our study (100-200 μM; 1-2 hrs) are sufficient to inhibit the Arp2/3 complex in mammalian cells, yet not high enough to cause any side

effects or affect cell viability. Thus, CK-666 and its analogues represent a powerful approach for studying both the Arp2/3 complex and the actin cytoskeleton in living cells.

Here we observed that treatment of M-1 cells with CK-666 lowered the motility rate and reduced the number of the observed lamellipodia formation up to 90%. These results are consistent with the observation that depletion of Arp2 and Arp3 with shRNA leads to the formation of filopodia and linear actin-based protrusions (Nicholson-Dykstra and Higgs 2008). Our observation that inhibition of Arp2/3 complex destroys cell motility is consistent with the growing evidence that this complex is an important participant in cell migration processes. It has also been shown to be involved in the migration of fibroblast monolayers during wound-healing (Magdalena et al. 2003;Warren et al. 2002). Moreover, the Arp2/3 complex was found in cellular regions characterized by dynamic actin filament activity such as lamellipodia and motile actin patches in yeast (Warren et al. 2002). Transverse arcs, which are stress fibers not directly anchored to substrate, are generated by endwise annealing of myosin bundles and Arp2/3-nucleated actin bundles at the lamella (Hotulainen and Lappalainen 2006).

The Arp2/3 complex has been shown to play a critical role in cancer. The invasion of cancer cells into the surrounding tissue is an initial step in metastasis, which is the leading cause of death from cancer. When cancer cells gain the ability to move, they break away from the primary tumor and colonize elsewhere in the body. Therefore, cancer cells generate cellular protrusions at the front of cells to facilitate the movement process. The driving force for membrane protrusion is localized polymerization of the actin filaments (Yamaguchi and Condeelis 2007) during which various membrane structures such as lamellipodia and invadopodia are formed. This process requires activation of the Arp2/3 complex to nucleate the formation of new actin filaments that exert a protrusive force on the membrane. Preventing metastasis, the spread of cancer cells from a primary tumor to a secondary site, might be an important therapeutic approach to cancer treatment. For example, renal collecting duct carcinoma arises from the epithelium of the collecting duct tubules within the renal medulla, which then secondarily invades the renal cortex (Carter et al. 1992;Zagoria et al. 1990). A number of groups have examined the role of the Arp2/3 complex in lamellipodia assembly and cell motility using genetic and molecular approaches, such as siRNA and shRNA targeted against Arp2/3 complex subunits (Gomez et al. 2007;Steffen et al. 2006;Di Nardo A. et al. 2005), and the use of the mutants of Arp2/3 interacting proteins (Gupton et al. 2005;Shao et al. 2006;Strasser et al. 2004). Results of these studies were interpreted by the authors in different ways. For instance, some authors demonstrated that loss of Arp2/3 complex components has little or no effect on general cell morphology, motility or viability (Di Nardo A. et al. 2005). Di Nardo et al. showed that knocking down expression of subunits of Arp2/3 complex by 90% had little impact on lamellipodia, and therefore Arp2/3 complex is not required for lamellipodia formation. However, 10% of Arp2/3 complex would still be around in the cells and such a knock down experiment cannot be interpreted unequivocally, although the data is sound. Our results show a significant decrease in M-1 cells motility after inhibition of the Arp2/3 complex, which is in accordance with Suraneni et al and Wu et al (Suraneni P. et al. 2012;Wu C. et al. 2012).

The Bellini duct carcinoma (BDC), which is a rare and aggressive primary renal neoplasm, forms in the principal cells lining the distal collecting duct epithelium (Verdorfer et al. 1998) and distal renal tubules (Auguet et al. 2000;Dobronski et al. 1999). Despite the fact that collecting duct BDC comprises 1% of all diagnosed duct renal cell cancer, about 50% of patients with localized disease progress with distant metastasis. Currently there is no effective therapy for metastatic collecting duct carcinoma, and surgical removal of these metastases are often associated with a poor prognosis. Thus, CK-666 and its analogs might be promising pharmacological tools for future development of the approaches allowing

targeted or local drug delivery, for instance, by intratumoral injection approach at the early stages of cancer progression.

To summarize, we have found that the use of direct and non-toxic inhibitors of the Arp2/3 complex may be a beneficial treatment option for various metastatic cancers, which rely on tumor cell motility and invasion that are regulated by dynamics of the cortical actin cytoskeleton. CK-666 and CK-869 studied in this research showed high potency to inhibit the Arp2/3 complex, which decreased cell motility rate and inhibited formation of the lamellipodia. The ability to inhibit the formation of the Arp2/3 complex and effect lamellipodia formation not only provides insight into the mechanisms regulating cell migration in the kidney, but it also provides rationale for investigating these mechanisms in cancer metastases in other organ systems.

Supplementary Material

Refer to Web version on PubMed Central for supplementary material.

Acknowledgments

The authors would like to acknowledge Dr. Grigoriy Stein (Institute of Cytology RAS) for help with microscopy experiments and sincerely thank Vladislav Levchenko (Medical College of Wisconsin) for help with the MTT cytotoxicity assay and critical reading of the manuscript. We also acknowledge the help of Glenn Slocum andbrad Endres (Medical College of Wisconsin) for helpful discussion and correction of the manuscript. Laboratory of Dr. A.N. Tomilin (Institute of Cytology RAS, St. Petersburg) is recognized for sharing the antibodies for immunofluorescence. This research was supported by R01HL108880 from the National Heart, Lung, and Blood Institute and the American Diabetes Association grant 1-10-BS-168 (to AS), Russian Foundation for Basic Research grant RFBR-13-04-00700 and the Molecular and Cell Biology Program of the Russian Academy of Sciences (to YAN and DVI), and the OPTEC research grant (to DVI and LSS).

Reference List

Auguet T, Molina JC, Lorenzo A, Vila J, Sirvent JJ, Richart C. Synchronus renal cell carcinoma and Bellini duct carcinoma: a case report on a rare coincidence. World J Urol. 2000; 18:449–451. [PubMed: 11204268]

Baggett AW, Cournia Z, Han MS, Patargias G, Glass AC, Liu SY, Nolen BJ. Structural characterization and computer-aided optimization of a small-molecule inhibitor of the arp2/3 complex, a key regulator of the actin cytoskeleton. ChemMedChem. 2012; 7:1286–1294. [PubMed: 22623398]

Bosse T, Ehinger J, Czuchra A, Benesch S, Steffen A, Wu X, Schloen K, Niemann HH, Scita G, Stradal TE, Brakebusch C, Rottner K. Cdc42 and phosphoinositide 3- kinase drive Rac-mediated actin polymerization downstream of c-Met in distinct and common pathways. Mol Cell Biol. 2007; 27:6615–6628. [PubMed: 17682062]

Bryant DM, Mostov KE. From cells to organs: building polarized tissue. Nat Rev Mol Cell Biol. 2008; 9:887–901. [PubMed: 18946477]

Cantarella C, Sepe L, Fioretti F, Ferrari MC, Paolella G. Analysis and modelling of motility of cell populations with MotoCell. BMC Bioinformatics. 2009; 10(Suppl 12):S12. [PubMed: 19828072]

Carter MD, Tha S, McLoughlin MG, Owen DA. Collecting duct carcinoma of the kidney: a case report and review of the literature. J Urol. 1992; 147:1096–1098. [PubMed: 1552595]

Chen Z, Borek D, Padrick SB, Gomez TS, Metlagel Z, Ismail AM, Umetani J, Billadeau DD, Otwinowski Z, Rosen MK. Structure and control of the actin regulatory WAVE complex. Nature. 2010; 468:533–538. [PubMed: 21107423]

Collins A, Warrington A, Taylor KA, Svitkina T. Structural Organization of the Actin Cytoskeleton at Sites of Clathrin-Mediated Endocytosis. Curr Bio. 2011

Di Nardo A, Cicchetti G, Falet H, Hartwig JH, Stossel TP, Kwiatkowski DJ. Arp2/3 complex-deficient mouse fibroblasts are viable and have normal leading-edge actin structure and function. Proc Natl Acad Sci U S A. 2005; 102:16263–16268. [PubMed: 16254049]

Dobronski P, Czaplicki M, Kozminska E, Pykalo R. Collecting (Bellini) duct carcinoma of the kidney--clinical, radiologic and immunohistochemical findings. Int Urol Nephrol. 1999; 31:601–609. [PubMed: 10755350]

Duleh SN, Welch MD. WASH and the Arp2/3 complex regulate endosome shape and trafficking. Cytoskeleton (Hoboken). 2010; 67:193–206. [PubMed: 20175130]

Firat-Karalar EN, Welch MD. New mechanisms and functions of actin nucleation. Curr Opin Cell Biol. 2011; 23:4–13. [PubMed: 21093244]

Gomez TS, Kumar K, Medeiros RB, Shimizu Y, Leibson PJ, Billadeau DD. Formins regulate the actin-related protein 2/3 complex-independent polarization of the centrosome to the immunological synapse. Immunity. 2007; 26:177–190. [PubMed: 17306570]

Gu J, Tamura M, Pankov R, Danen EH, Takino T, Matsumoto K, Yamada KM. Shc and FAK differentially regulate cell motility and directionality modulated by PTEN. J Cell Biol. 1999; 146:389–403. [PubMed: 10427092]

Gupton SL, Anderson KL, Kole TP, Fischer RS, Ponti A, Hitchcock-DeGregori SE, Danuser G, Fowler VM, Wirtz D, Hanein D, Waterman-Storer CM. Cell migration without a lamellipodium: translation of actin dynamics into cell movement mediated by tropomyosin. J Cell Biol. 2005; 168:619–631. [PubMed: 15716379]

Hetrick B, Han MS, Helgeson LA, Nolen BJ. Small Molecules CK-666 and CK-869 Inhibit Actin-Related Protein 2/3 Complex by Blocking an Activating Conformational Change. Chem Biol. 2013; 20:701–712. [PubMed: 23623350]

Hotulainen P, Lappalainen P. Stress fibers are generated by two distinct actin assembly mechanisms in motile cells. J Cell Biol. 2006; 173:383–394. [PubMed: 16651381]

Ilatovskaya DV, Pavlov TS, Levchenko V, Negulyaev YA, Staruschenko A. Cortical actin binding protein cortactin mediates ENaC activity via Arp2/3 complex. The FASEB Journal. 2011; 25:2688–2699.

Karpushev AV, Ilatovskaya DV, Staruschenko A. The actin cytoskeleton and small G protein RhoA are not involved in flow-dependent activation of ENaC. BMC Res Notes. 2010; 3:210. [PubMed: 20663206]

Karpushev AV, Levchenko V, Ilatovskaya DV, Pavlov TS, Staruschenko A. Novel Role of Rac1/WAVE Signaling Mechanism in Regulation of the Epithelial Na+ Channel. Hypertension. 2011; 57:996–1002. [PubMed: 21464391]

Kinoshita T, Nohata N, Watanabe-Takano H, Yoshino H, Hidaka H, Fujimura L, Fuse M, Yamasaki T, Enokida H, Nakagawa M, Hanazawa T, Okamoto Y, Seki N. Actinrelated protein 2/3 complex subunit 5 (ARPC5) contributes to cell migration and invasion and is directly regulated by tumor-suppressive microRNA-133a in head and neck squamous cell carcinoma. Int J Oncol. 2012; 40:1770–1778. [PubMed: 22378351]

Lebensohn AM, Kirschner MW. Activation of the WAVE complex by coincident signals controls actin assembly. Mol Cell. 2009; 36:512–524. [PubMed: 19917258]

Machesky LM, Atkinson SJ, Ampe C, Vandekerckhove J, Pollard TD. Purification of a cortical complex containing two unconventional actins from Acanthamoeba by affinity chromatography on profilin-agarose. J Cell Biol. 1994; 127:107–115. [PubMed: 7929556]

Machesky LM, Insall RH. Scar1 and the related Wiskott-Aldrich syndrome protein, WASP, regulate the actin cytoskeleton through the Arp2/3 complex. Curr Biol. 1998; 8:1347–1356. [PubMed: 9889097]

Magdalena J, Millard TH, Etienne-Manneville S, Launay S, Warwick HK, Machesky LM. Involvement of the Arp2/3 complex and Scar2 in Golgi polarity in scratch wound models. Mol Biol Cell. 2003; 14:670–684. [PubMed: 12589062]

Nakamura Y, Wood CL, Patton AP, Jaafari N, Henley JM, Mellor JR, Hanley JG. PICK1 inhibition of the Arp2/3 complex controls dendritic spine size and synaptic plasticity. EMBO J. 2011; 30:719–730. [PubMed: 21252856]

Naray-Fejes-Toth A, Helms MN, Stokes JB, Fejes-Toth G. Regulation of sodium transport in mammalian collecting duct cells by aldosterone-induced kinase, SGK1: structure/function studies. Mol Cell Endocrinol. 2004; 217:197–202. [PubMed: 15134818]

Nicholson-Dykstra SM, Higgs HN. Arp2 depletion inhibits sheet-like protrusions but not linear protrusions of fibroblasts and lymphocytes. Cell Motil Cytoskeleton. 2008; 65:904–922. [PubMed: 18720401]

Nolen BJ, Tomasevic N, Russell A, Pierce DW, Jia Z, McCormick CD, Hartman J, Sakowicz R, Pollard TD. Characterization of two classes of small molecule inhibitors of Arp2/3 complex. Nature. 2009; 460:1031–1034. [PubMed: 19648907]

Peleg B, Disanza A, Scita G, Gov N. Propagating cell-membrane waves driven by curved activators of actin polymerization. PLoS One. 2011; 6:e18635. [PubMed: 21533032]

Pollard TD. Regulation of actin filament assembly by Arp2/3 complex and formins. Annu Rev Biophys Biomol Struct. 2007; 36:451–477. [PubMed: 17477841]

Robinson RC, Turbedsky K, Kaiser DA, Marchand JB, Higgs HN, Choe S, Pollard TD. Crystal structure of Arp2/3 complex. Science. 2001; 294:1679–1684. [PubMed: 11721045]

Rouiller I, Xu XP, Amann KJ, Egile C, Nickell S, Nicastro D, Li R, Pollard TD, Volkmann N, Hanein D. The structural basis of actin filament branching by the Arp2/3 complex. J Cell Biol. 2008; 180:887–895. [PubMed: 18316411]

Saarikangas J, Zhao H, Lappalainen P. Regulation of the actin cytoskeletonplasma membrane interplay by phosphoinositides. Physiol Rev. 2010; 90:259–289. [PubMed: 20086078]

Sarmiento C, Wang W, Dovas A, Yamaguchi H, Sidani M, El-Sibai M, Desmarais V, Holman HA, Kitchen S, Backer JM, Alberts A, Condeelis J. WASP family members and formin proteins coordinate regulation of cell protrusions in carcinoma cells. J Cell Biol. 2008; 180:1245–1260. [PubMed: 18362183]

Shao D, Forge A, Munro PM, Bailly M. Arp2/3 complex-mediated actin polymerisation occurs on specific pre-existing networks in cells and requires spatial restriction to sustain functional lamellipod extension. Cell Motil Cytoskeleton. 2006; 63:395–414. [PubMed: 16619224]

Soderling SH. Grab your partner with both hands: cytoskeletal remodeling by Arp2/3 signaling. Sci Signal. 2009; 2:e5.

Spillane M, Ketschek A, Jones SL, Korobova F, Marsick B, Lanier L, Svitkina T, Gallo G. The actin nucleating Arp2/3 complex contributes to the formation of axonal filopodia and branches through the regulation of actin patch precursors to filopodia. Dev Neurobiol. 2011

Steffen A, Faix J, Resch GP, Linkner J, Wehland J, Small JV, Rottner K, Stradal TE. Filopodia formation in the absence of functional. Mol Biol Cell. 2006; 17:2581–2591. [PubMed: 16597702]

Strasser GA, Rahim NA, VanderWaal KE, Gertler FB, Lanier LM. Arp2/3 is a negative regulator of growth cone translocation. Neuron. 2004; 43:81–94. [PubMed: 15233919]

Sun CX, Magalhaes MA, Glogauer M. Rac1 and Rac2 differentially regulate actin free barbed end formation downstream of the fMLP receptor. J Cell Biol. 2007; 179:239–245. [PubMed: 17954607]

Sun SC, Wang ZB, Xu YN, Lee SE, Cui XS, Kim NH. Arp2/3 complex regulates asymmetric division and cytokinesis in mouse oocytes. PLoS One. 2011; 6:e18392. [PubMed: 21494665]

Suraneni P, Rubinstein B, Unruh JR, Durnin M, Hanein D, Li R. The Arp2/3 complex is required for lamellipodia extension and directional fibroblast cell migration. J Cell Biol. 2012; 197:239–251. [PubMed: 22492726]

Verdorfer I, Culig Z, Hobisch A, Bartsch G, Hittmair A, Duba HC, Erdel M. Characterisation of a collecting duct carcinoma by cytogenetic analysis and comparative genomic hybridisation. Int J Oncol. 1998; 13:461–464. [PubMed: 9683779]

Volkmann N, Amann KJ, Stoilova-McPhie S, Egile C, Winter DC, Hazelwood L, Heuser JE, Li R, Pollard TD, Hanein D. Structure of Arp2/3 complex in its activated state and in actin filament branch junctions. Science. 2001; 293:2456–2459. [PubMed: 11533442]

Wang W, Goswami S, Lapidus K, Wells AL, Wyckoff JB, Sahai E, Singer RH, Segall JE, Condeelis JS. Identification and testing of a gene expression signature of invasive carcinoma cells within primary mammary tumors. Cancer Res. 2004; 64:8585–8594. [PubMed: 15574765]

Warren DT, Andrews PD, Gourlay CW, Ayscough KR. Sla1p couples the yeast endocytic machinery to proteins regulating actin dynamics. J Cell Sci. 2002; 115:1703–1715. [PubMed: 11950888]

Watanabe S, Okawa K, Miki T, Sakamoto S, Morinaga T, Segawa K, Arakawa T, Kinoshita M, Ishizaki T, Narumiya S. Rho and anillin-dependent control of mDia2 localization and function in cytokinesis. Mol Biol Cell. 2010; 21:3193–3204. [PubMed: 20660154]

Weed SA, Karginov AV, Schafer DA, Weaver AM, Kinley AW, Cooper JA, Parsons JT. Cortactin localization to sites of actin assembly in lamellipodia requires interactions with F-actin and the Arp2/3 complex. J Cell Biol. 2000; 151:29–40. [PubMed: 11018051]

Weed SA, Parsons JT. Cortactin: coupling membrane dynamics to cortical actin assembly. Oncogene. 2001; 20:6418–6434. [PubMed: 11607842]

Wilson PD. Apico-basal polarity in polycystic kidney disease epithelia. Biochim Biophys Acta. 2011

Wu C, Asokan SB, Berginski ME, Haynes EM, Sharpless NE, Griffith JD, Gomez SM, Bear JE. Arp2/3 is critical for lamellipodia and response to extracellular matrix cues but is dispensable for chemotaxis. Cell. 2012; 148:973–987. [PubMed: 22385962]

Yamaguchi H, Condeelis J. Regulation of the actin cytoskeleton in cancer cell migration and invasion. Biochim Biophys Acta. 2007; 1773:642–665. [PubMed: 16926057]

Yamaguchi H, Lorenz M, Kempiak S, Sarmiento C, Coniglio S, Symons M, Segall J, Eddy R, Miki H, Takenawa T, Condeelis J. Molecular mechanisms of invadopodium formation: the role of the N-WASP-Arp2/3 complex pathway and cofilin. J Cell Biol. 2005; 168:441–452. [PubMed: 15684033]

Zagoria RJ, Wolfman NT, Karstaedt N, Hinn GC, Dyer RB, Chen YM. CT features of renal cell carcinoma with emphasis on relation to tumor size. Invest Radiol. 1990; 25:261–266. [PubMed: 2332312]

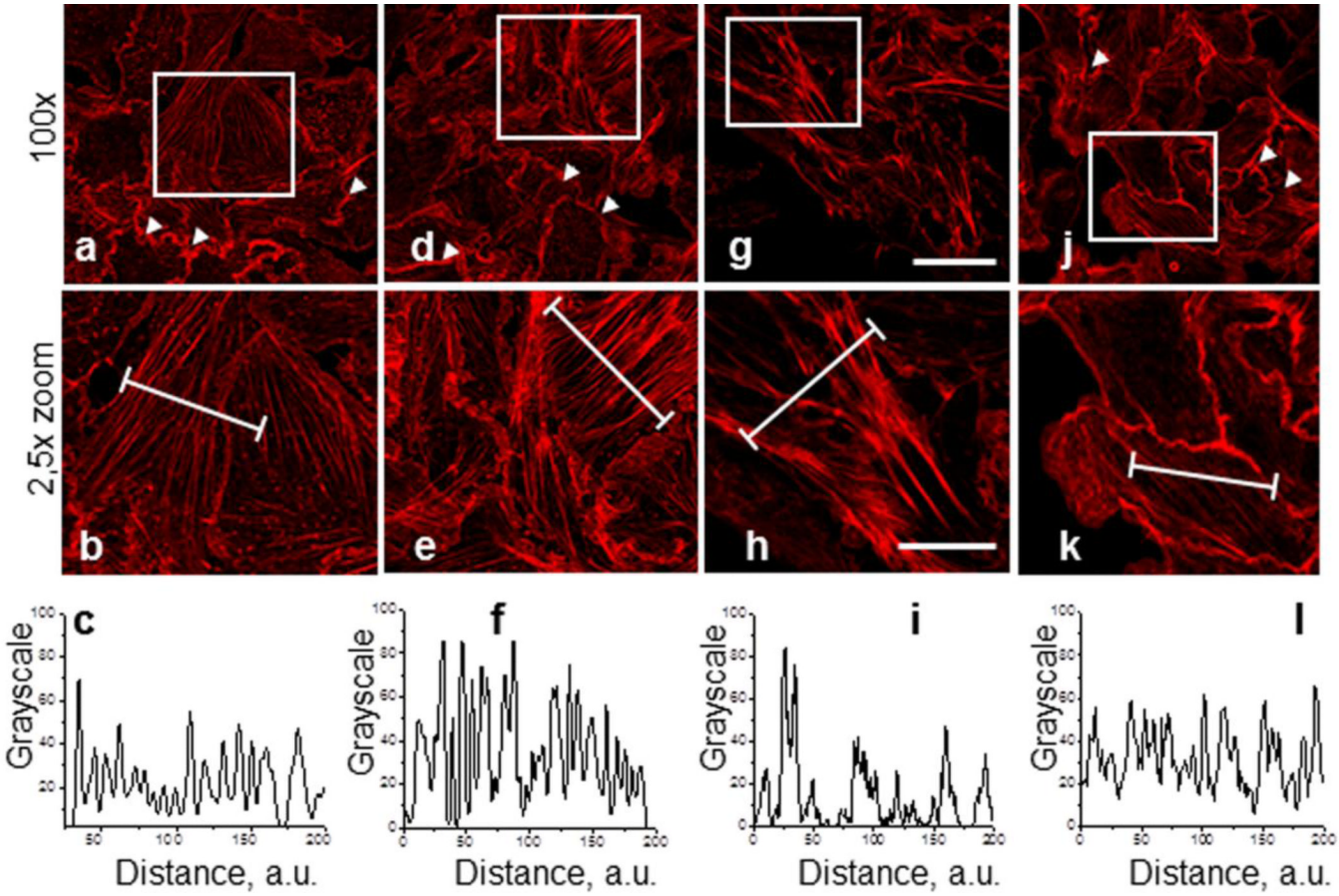

Fig. 1.

Effect of the Arp2/3 complex inhibition with CK-666 and CK-689 on actin cytoskeleton organization in M-1 epithelial cells. M-1 cells were pretreated with vehicle (**a)** CK-0499666 (CK-666) in concentrations of 100 μM and 200 μM for 2 hrs (**d**), and **g**, respectively, or CK-689 (**j**, 2 hrs, 200 μM). Corresponding close-up images are shown under full images (**b, e, h**, and **k** respectively). Images were taken from M-1 cells stained with rhodamine-phalloidin to visualize actin microfilaments. Scale bar is common for all the images of the row and is 25 and 10 μm for upper and lower rows, respectively. Bottom row (**c, f, I, l**) demonstrates relative fluorescence across a region of interest (white lines in correcponding close-up images).

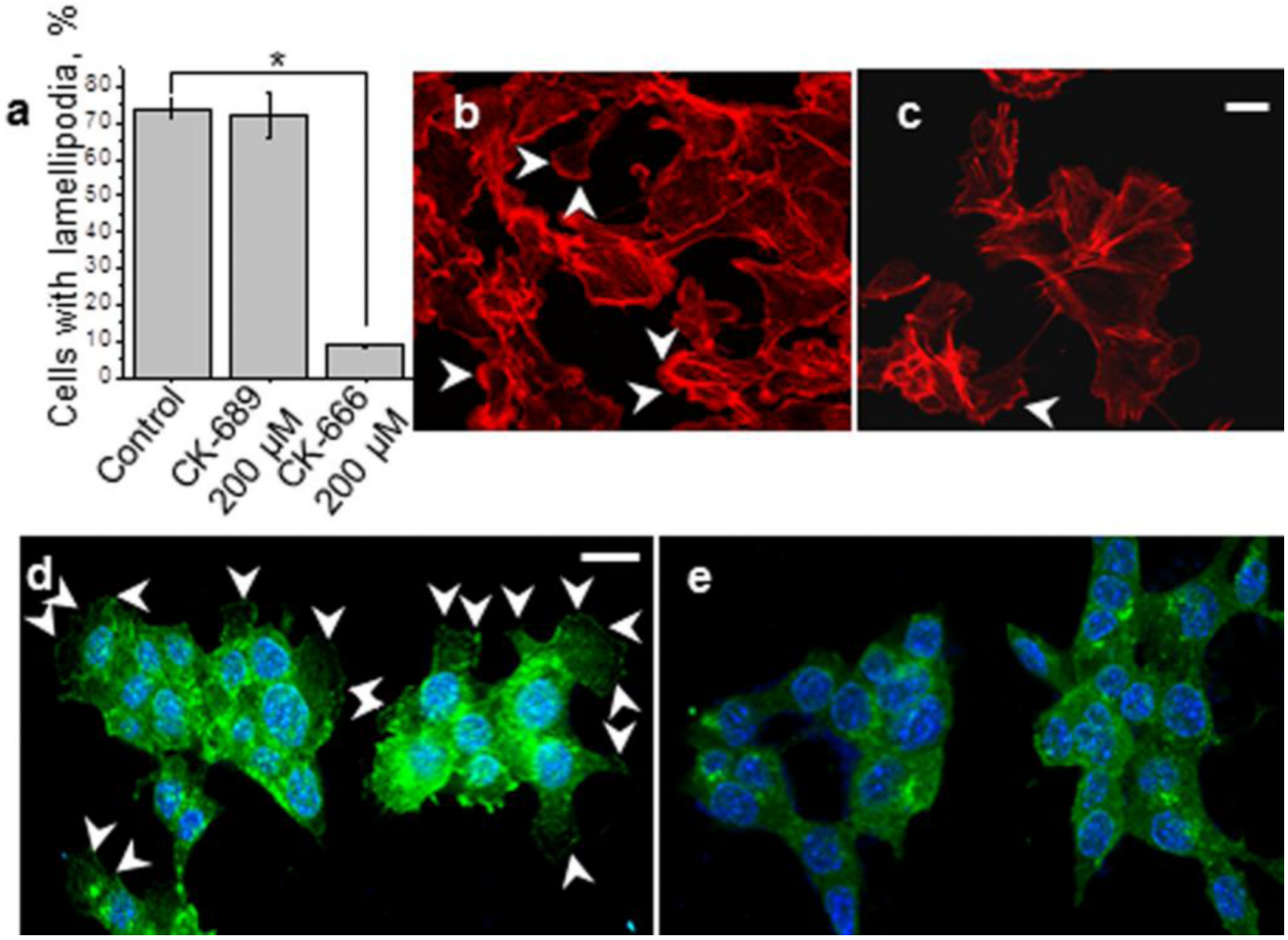

Fig. 2.

The effect of Arp2/3 complex inhibition on lamellipodia formation in M-1 cells. (**a**) The number of lamellipodia in M-1 cells treated with 200 μM CK-689 or CK-666 for 2 hrs. The percent changes in lamellipodia numbers were calculated from at least 6 fields of view, a representative field of view used in these calculations is shown in (**b** and **c** for untreated cells and cells treated with 100 μM CK-666 for 2 h, respectively); white arrowheads point out lamellipodia. Immunofluorescent staining of M-1 cells with anti-cortactin antibodies to visualize lamellipodia before (control, **d**) and after incubation with 100 μM CK-666 for 2 hrs (**e**). Lamellipodia are marked with white arrowheads. Scale bar shown in **b** and **e** is 10 μm. Lamellipodia were measured from at least 25 cells from 3 samples of each of 2 different experiments.

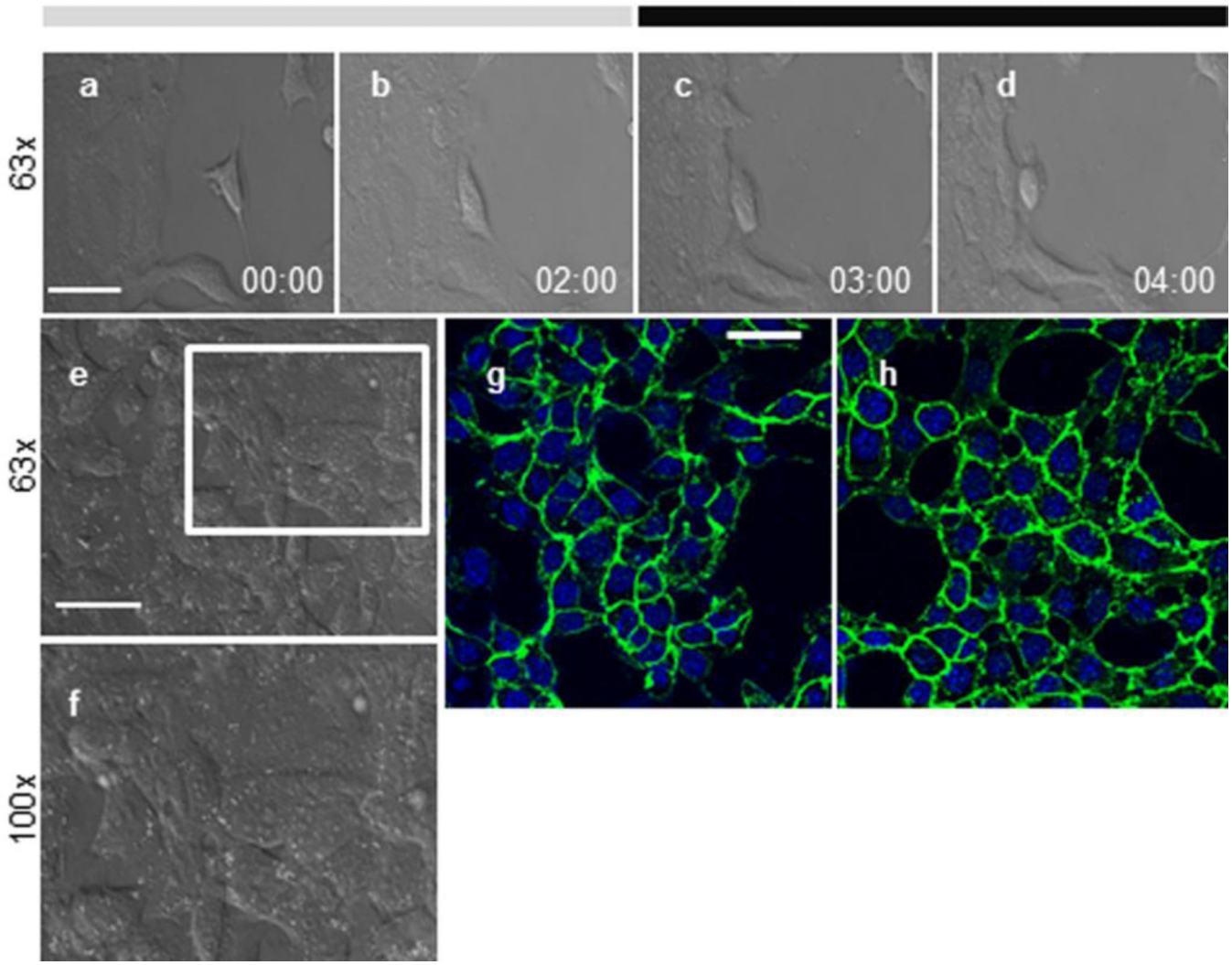

Fig. 3.

Effect of CK-666 on M-1 cell motility and monolayer integrity. (**a-d**) Shown are representative time series images of the motile M-1 cells: before treatment (**a**), after first 2 hrs in control (vehicle, **b**), 1 hr (**c**) and 2 hrs (**d**) after treatment with 200 μM CK-666. (**e,f**), Morphology of the M-1 cells seeded 90 % confluence was monitored for 2 hrs time periods before and after treatment with 200 μM of CK666. Shown is a representative image taken after treatment with CK-666 for 2 hrs at 63x (**e**) and a close-up image at 100x (**f**). (**g,h**), Immunofluorescent staining of M-1 cells with anti-β-catenin antibodies before (control, **g**) and after incubation with CK-666 for 2 hrs (**h**). Scale bar shown in is 25 μm.

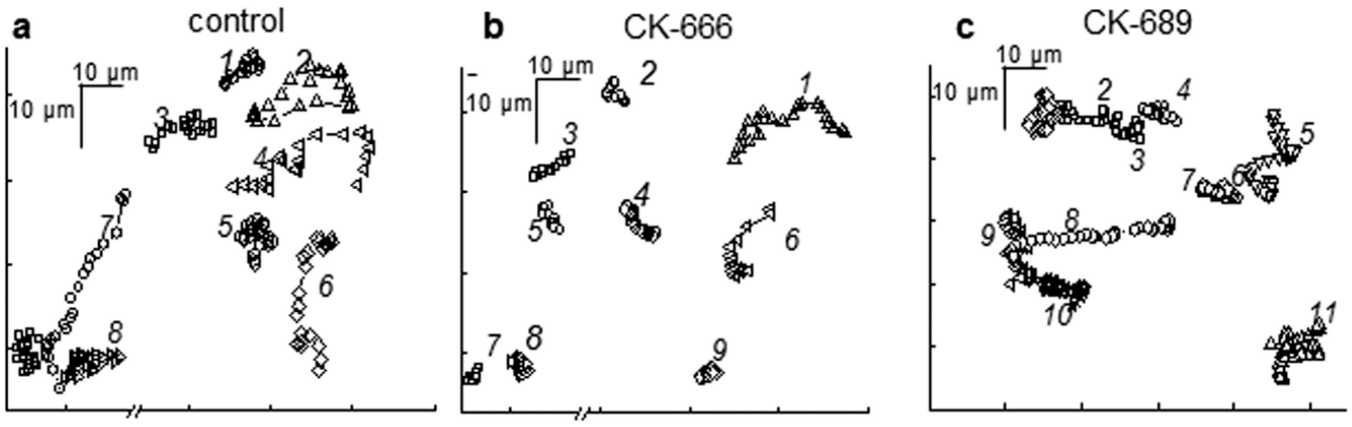

Fig. 4.

Representative motility tracks of the M-1 cell line after inhibition of the Arp2/3 complex with CK-666. Shown are the examples of cell tracks over 2 hrs interval; cells were chosen from the coverslips treated with vehicle (**a**, control), CK-666 (**b**) and CK689 (**c**) in concentrations of 200 μM.

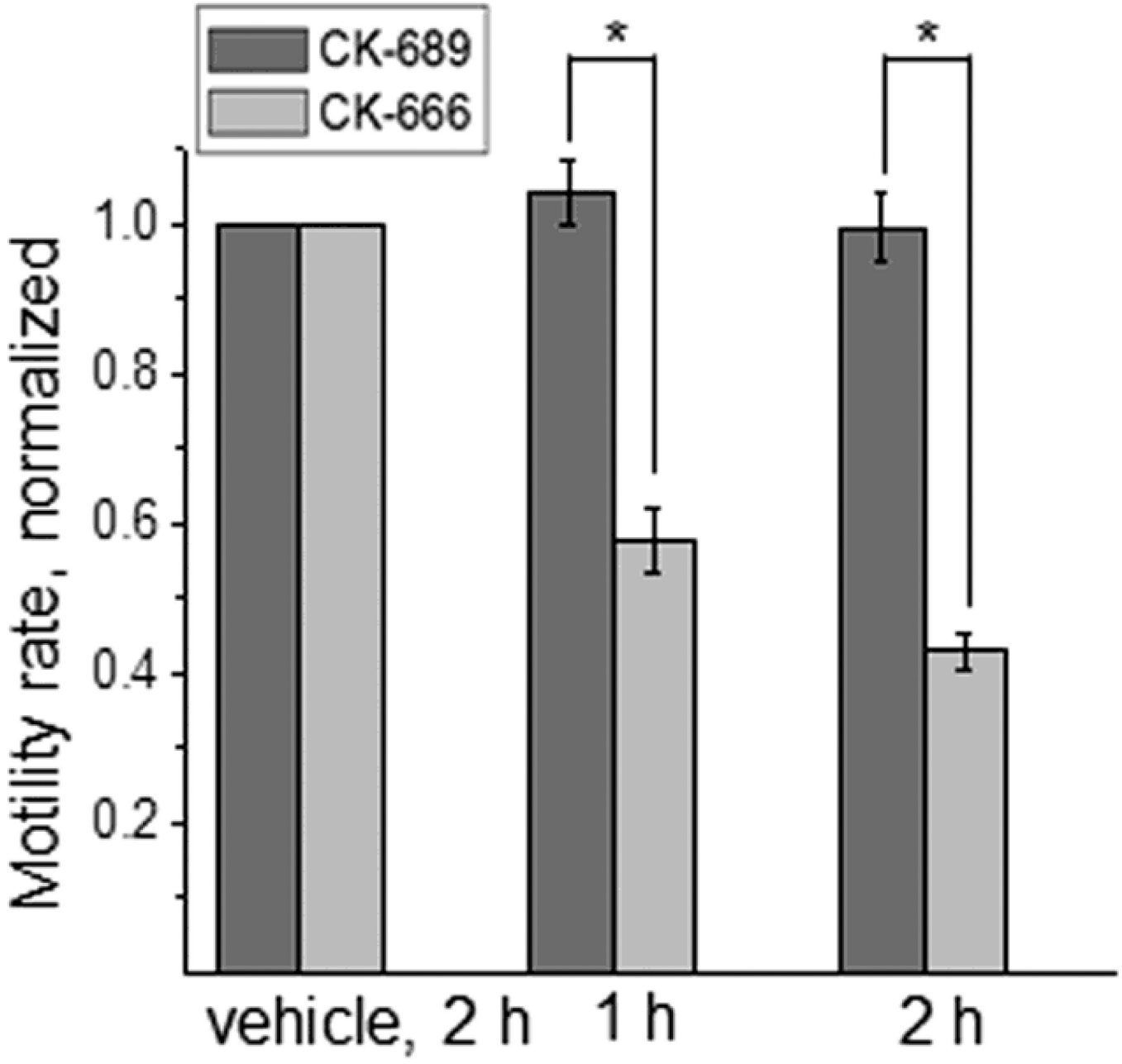

Fig. 5.

CK-666 treatment significantly decreased the motility of M-1 cells without any effect on the migration characteristics. Shown is the normalized motility rate after treatment with CK-666 and inactive analog CK-689. The motility rate was calculated from at least 25 cells for each bar, the experiments were repeated at least 3 times. Asterisk denotes $P \leq 0.005$.

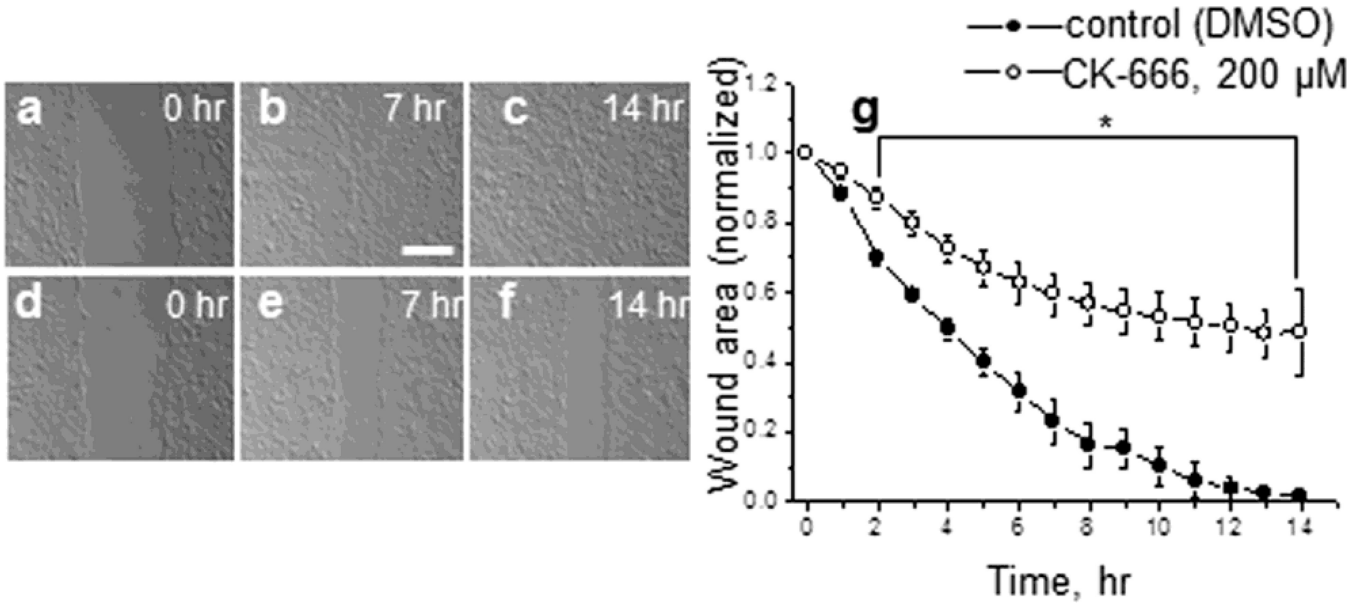

Fig. 6.

Effects of CK-666 on wound healing in M-1 cells' monolayer. Wound-healing montage of M-1 cells' treated with DMSO (control, **a-b-c**) and 200 μM of CK-666 (**d-e-f**) for up to 14 hrs. Shown are images from three different time points. Scale bar shown is 100 μm. (**g**), Quantification of the wound area (normalized to the starting point at 0 hrs) as a function of time. Plots show mean wound region area and SEM from up to 5 different wounds from 3 independent experiments throughout time. Asterisk denotes $P \leq 0.005$.